Available online at www.sciencedirect.com

SCIENCE DIRECT®

Surface & Coatings Technology 188–189 (2004) 299–306

SURFACE & COATINGS TECHNOLOGY

www.elsevier.com/locate/surfcoat

Plasma enhanced surface treatments using electron beam-generated plasmas

D. Leonhardt*, C. Muratore, S.G. Walton, R.A. Meger

Naval Research Laboratory, Plasma Physics Division, Washington, DC 20375, United States

Available online 19 October 2004

Abstract

NRL has developed a 'large area plasma processing system' (LAPPS) utilizing a high energy (~2 keV) modulated electron beam to drive the plasma ionization. This system has been shown to be (1) efficient at producing plasma in any gas composition, (2) capable of producing low temperature plasma electrons (<0.5 eV) in high densities (10^9–10^{12} cm^{-3}) and (3) scalable to large area (square meters). In this work, the progress of a number of applications using LAPPS is discussed. Nitride growth in stainless steel was investigated, which demonstrated high rates (up to 20 $\mu m/h^{1/2}$) at low temperatures (≤462 °C). Complementary mass spectrometry showed that the nitriding results correlated to the flux of atomic ions delivered to the substrate. LAPPS was also combined with magnetron sputtering sources to form hybrid systems for surface pretreatments of polymers for metallization and thin film deposition of nitrides. In these systems, Teflon® substrates pretreated with an oxygen LAPPS exposure demonstrated a significant increase in copper and aluminum film adhesion compared to untreated substrates, with the dominant factor believed to be the changed surface morphology. The simultaneous operation of LAPPS with a titanium magnetron sputter source increased the growth of the ⟨200⟩ orientation in TiN films, due to the increased atomic nitrogen ion flux. Additional LAPPS systems are also discussed.
© 2004 Elsevier B.V. All rights reserved.

Keywords: Nitriding; PACVD; Pulsed; Reactive Sputtering; Magnetron; E-beam Generated Plasma

1. Introduction

Conventional plasma discharges used in surface modification applications directly heat electrons with externally applied electromagnetic fields to ionize the gas. A significant amount of input power is therefore lost to low energy (0–10 eV) gas excitation processes rather than ionization or dissociation processes (10–20 eV) that produce the desired reactive plasma species. Additionally, plasmas sustained by heated electrons require electron temperatures of multiple electron volts, which generally translate to a plasma environment of high plasma potentials (>10 V), sheath drops and ion isotropy at surfaces. However when a high energy beam of electrons passes through a gas, its dominant process is ionization of the gas followed by dissociation and finally excitation. The direct ionization mechanism makes the plasma production process extremely efficient and easily scalable to large areas (square meters) when compared to conventional plasma discharges. The resultant plasmas, which are not relying on the plasma electrons to initiate ionization, have low electron temperatures and plasma potentials making them desirable for many surface modification applications.

Fernsler et al. [1] and Manheimer et al. [2] have discussed the detailed physics behind the plasma production mechanisms from electron beams, which agree with experimental in situ measurements [3,4]. More recently, a broader view of e-beam-generated plasmas was presented [5] to illustrate both the fundamental aspects and the range of plasma source configurations being investigated for various applications. This paper reports on the recent experimental progress of various applications with electron-beam-generated plasmas and their incorporation into multiple plasma source systems that are being pursued for materials' modification. These applications include the nitriding of stainless steel, surface

* Corresponding author. Tel.: +1 202 767 7532; fax: +1 202 767 3553.
E-mail address: darrin@ccs.nrl.navy.mil (D. Leonhardt).

0257-8972/$ - see front matter © 2004 Elsevier B.V. All rights reserved.
doi:10.1016/j.surfcoat.2004.08.195

activation (and subsequent metallization) of fluoropolymer material, and thin film deposition of metal nitrides.

2. Experimental arrangements

For all experiments discussed in this paper, a plasma 'layer' was used as discussed previously [6]. Briefly, a sheet of high energy electrons was produced by a linear hollow cathode to generate the plasma layer. The hollow cathode was nominally driven by −2 kV, 2 ms pulses at 50% duty factors, with typical currents of 0.1–1 mA/cm^2, depending on the application. No attempts were made to optimize the processes by varying the plasma's duty factor. The electron beam (e-beam) was accelerated out from the hollow channel and skimmed by an aperture in a grounded stainless steel anode to set the geometric shape of the beam. The anode was located ≈5 cm in front of the cathode and contained a 1-cm-wide slot of the same length as the cathode (15–25 cm). An axial magnetic field provided by either Helmholtz coils or a segmented solenoid arrangement kept the beam profile planar. The electron beam was terminated at another stainless steel anode, which was >40 cm away from the slotted anode.

The arrangement of the plasma processing system is shown in Fig. 1. The processing stages (or substrate holder) were introduced laterally, to the 'face' of the plasma layer. Stages were constructed with grounded support structures, temperature control capabilities, and an electrically isolated electrode 11 cm in diameter that was recessed in a ceramic insulator. When magnetron sources were incorporated, they were located opposite the stage on the other side of the e-beam produced plasma and were not modulated (100% duty factors). Samples were ultrasonically cleaned in acetone and/or methanol then dried prior to being mounted in the vacuum chamber, typically 1.5 cm from the center of the beam channel.

Experiments were carried out in a variety of vacuum chambers. In every system, mass flow controllers were used for stable gas flow of 20–50 sccm and the high vacuum pump (turbomolecular or diffusion) was throttled with a manual valve or iris to set the system's operating pressure. All chambers were metal in construction and had base pressures below 2.6×10^{-4} Pa (2×10^{-6} Torr).

2.1. Plasma nitriding

These experiments are the subject of two recent articles [7,8] so only minimal detail will be given here. Samples approximately 5 cm^2 were cut from a 0.6 cm thick plate of 316 stainless steel and polished to a surface roughness of 0.020 μm. The e-beam generated plasma and −350 Vdc sample bias was initiated in 21.3 Pa of nitrogen and argon (88:12, respectively) as the sample process temperature (325–462 °C) was reached in 30 min. The processing stage temperature was then kept constant for and additional 6.5 h.

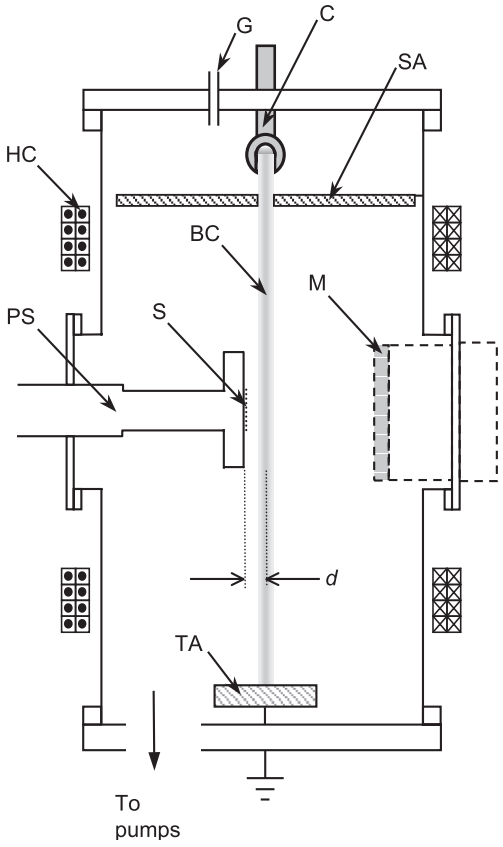

Fig. 1. Experimental arrangement for e-beam-generated processing system. System components are labeled as follows: (C) cathode; (G) gas feed; (SA) slotted anode; (HC) Helmholtz coils; (BC) e-beam channel and plasma; (S) substrate; (PS) processing stage; (M) additional magnetron source; and (d) distance from beam center to substrate surface.

After plasma exposure, the samples were allowed to cool in a nitrogen atmosphere then removed from vacuum, sectioned and sputter coated with titanium. The sections were then polished to 1 μm, etched in Marble's solution, polished again, and analyzed with a Vickers' microindenter microscope to determine the nitride layer thickness. Surface hardness was determined with an UMIS 2000 fitted with a diamond indenter.

2.2. Diagnostics

To characterize the plasma/surface interface in the nitriding system, the same operating conditions were set in a system where ion species were energy and mass resolved with a differentially pumped EQP300 Plasma Probe (Hiden Analytical) as discussed in Ref. [4]. The major differences between these measurements and the nitriding conditions were that a different vacuum chamber was used (base pressure below 1×10^{-5} Pa) and the sampling stage, which was similarly located 1.5 cm from the center of the beam channel. The EQP stage was smaller in diameter (5.7 cm) than the processing stage and contained a 20 μm sampling orifice, was not actively heated and was

electrically grounded. In order to obtain ion energy distributions due to a dc bias at the EQP electrode, the termination anode was biased to +100 Vdc to raise the plasma potential and thereby provide a comparable sheath drop at the grounded EQP stage. (The 100 Vdc level was used instead of the 350 Vdc level used in nitriding experiments to avoid spurious dc breakdowns around the non-insulated termination anode.)

2.3. Polymer pretreatment for metallization

For these experiments, two plasma systems were operated independently; the e-beam produced plasma for surface pretreatment followed by the PVD (sputter deposition) of the metal film. Thin (70 μm) Teflon® pieces roughly 4 cm^2 were masked with 5 mm wide Kapton® tape and mounted to the grounded processing stage. A sputter magnetron source with a 3 cm diameter aluminum or copper target was located 13 cm from the Teflon® substrate. The relative positions of the beam, magnetron target and substrate were independently set but not optimized. Plasma pretreatment consisted of operating the e-beam at a 20% duty factor in 6.7 Pa oxygen for 10 min of exposure time (over 50 min of elapsed time). After plasma pretreatment, the magnetron was operated in 2.4 Pa argon at 100 W to deposit ≈700 nm thick metal films. Comparisons between the metal film adhesion with and without plasma pretreatment were carried out through visual inspection and the AIMCAL 'Scotch® Tape Test' [9] to qualitatively test film adhesion. To examine the effects of oxygen plasma pretreatment on the substrate material alone, wetting tests and atomic force microscopy (AFM) were used to compare the surfaces of the treated and untreated samples. The wetting tests consisted of measuring the contact angle of a drop of distilled water on the surface and a Digital Instruments atomic force microscope was used for all AFM data in this work.

2.4. Titanium nitride deposition

A 15 cm diameter magnetron with a titanium target was mounted 7 cm from the processing stage to deposit thin films of titanium nitride (TiN) in an argon/nitrogen atmosphere. Silicon ⟨100⟩ substrates 2–3 cm^2 in size were cleaned by an e-beam generated plasma in 6 Pa argon with a dc bias −50 V to the stage, while heated to 250 °C over the course of 15 min. The temperature was stabilized an additional 3 min, then the magnetron target was powered to 800 W. After 2 min of operation in pure argon, 0.9 sccm of nitrogen was introduced into the chamber, resulting in no change of process pressure. Nitride deposition was then carried out with both plasma sources for 20 min with the substrate maintained at 250 °C and −50 Vdc. For comparison, films were grown with only the magnetron source for the same 20 min deposition time, keeping the average ion current to the sample stage the same as measured in the hybrid system (0.6 mA/cm^2) by minor (<2%) adjustments in the externally applied axial magnetic field. X-ray diffraction (XRD) using a Rigaku 15 kW system (with a Cu Kα source) and AFM were used to characterize the resultant TiN films.

3. Results

3.1. Plasma nitriding

The natural logarithm of the nitriding rate versus the inverse of process temperature is shown in Fig. 2. The nitrided layer thickness and plasma exposure time (50% of 7.0 h) were used to calculate reported nitriding rates, which were determined by assuming a diffusion-controlled growth rate proportional to the square root of the exposure time. The process activation energy (E_a) was determined from the Arrhenius relation ($\exp(-E_a/kT)$) and the linear least squares fit of the data in Fig. 2 resulted in an activation energy 1.4 eV/atom for this process. The hardness of all nitrided samples was measured at ≈15.5 GPa, compared to the untreated stainless steel surface of 2.6 GPa.

3.2. Diagnostics

The composition of the ion flux (see Ref. [8]) contained comparable amounts of molecular and atomic nitrogen ions up to 3 cm from the e-beam center. Fig. 3 shows the normalized ion energy distribution functions (IEDFs) acquired during the e-beam operation for the dominant molecular and atomic ion fluxes. For comparison, the insert shows the IEDFs with no external biasing. With no external bias, both ions showed narrow (<1 eV FWHM) low energy (0.8–2.5 eV) distributions, with the atomic ion having slightly higher maximum and most probable energies. The

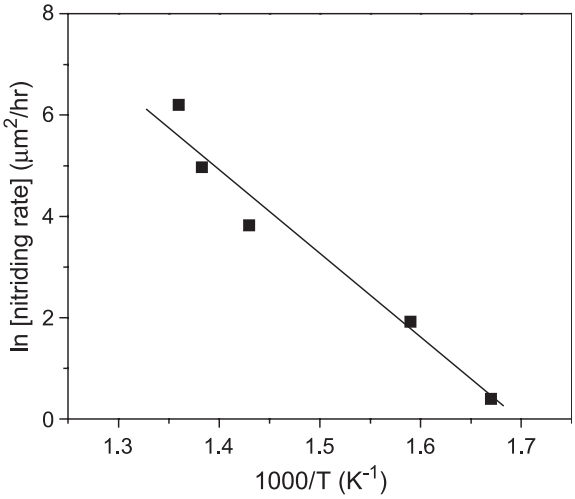

Fig. 2. Arrhenius plot of the measured stainless steel nitriding rate in an e-beam-generated plasma.

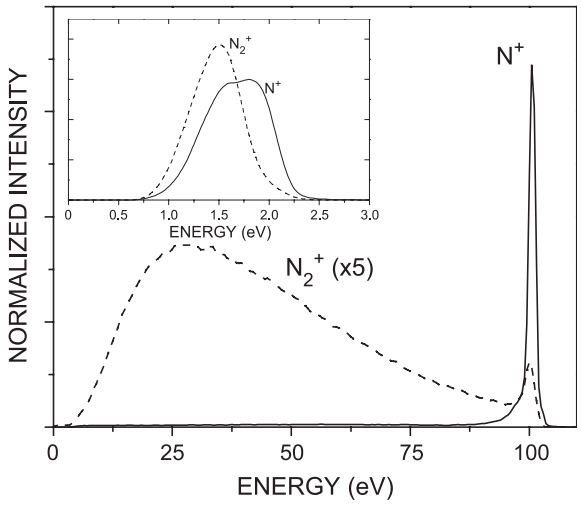

Fig. 3. Ion energy distributions of nitrogen species traversing an imposed 100 V sheath and with typical e-beam-generated plasma sheath (inset).

applied bias of 100 V shifted the atomic IEDF to approximately 100 eV, but the molecular ion showed a broad distribution spanning the entire energy range, with a most probable energy of 25 eV and a small secondary peak in energy at 100 eV.

Temporally resolved Langmuir probe data measured under similar conditions can be found elsewhere [3,6,10] for the plasmas discussed in this work. Steady-state plasma electron densities of $\approx 2\times10^{11}$ cm^{-3}, temperatures ≈ 0.4 eV, and plasma potentials of 3–5 V are typical for the molecular gases used in these experiments.

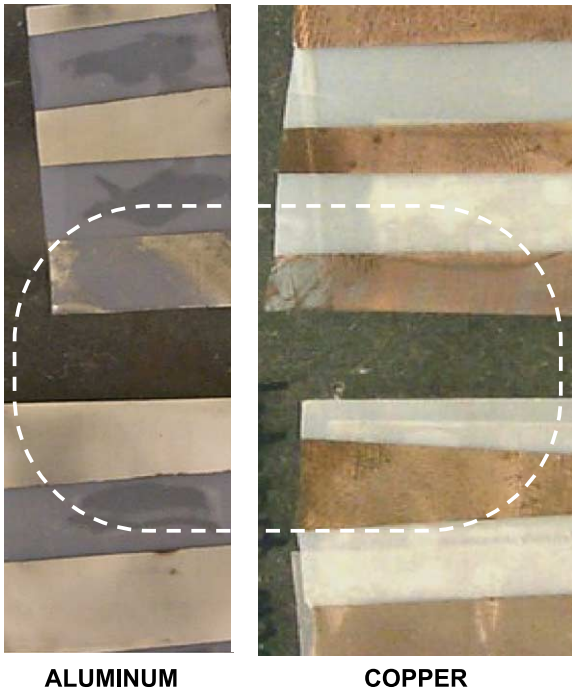

Fig. 4. Scotch® Tape test results of metal film deposition on Teflon® with e-beam-generated plasma pretreatment (top) and without (bottom).

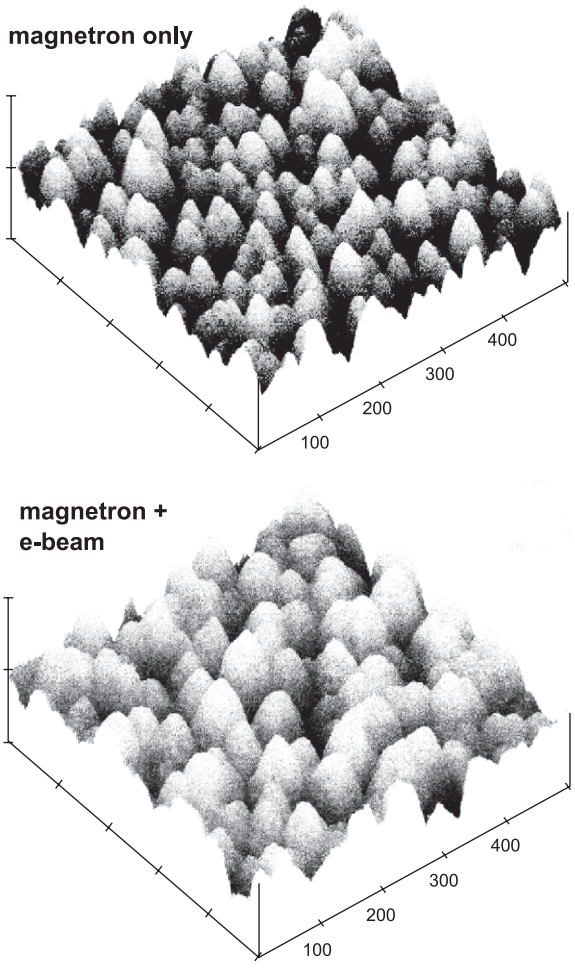

Fig. 5. AFM images of TiN films deposited by reactive sputtering with magnetron source without e-beam-generated plasma (top) and with the e-beam-generated plasma (bottom) between the magnetron and substrate.

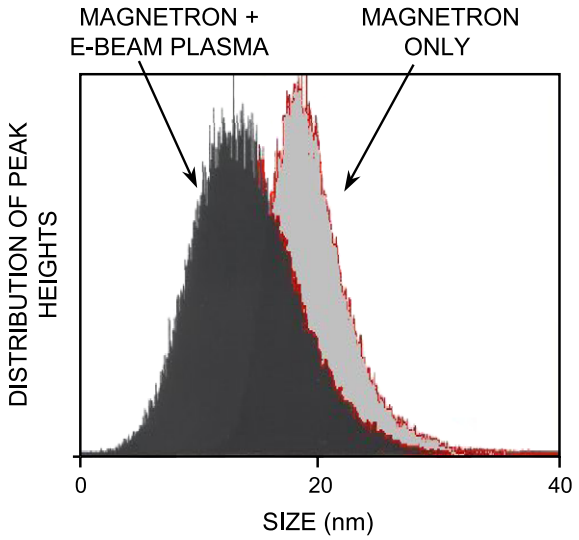

Fig. 6. Peak height distributions from AFM data for TiN grown films in the magnetron-only and e-beam produced plasma+magnetron systems.

3.3. Polymer pretreatment for metallization

Results of the AIMCAL Scotch® Tape tests are shown in Fig. 4, where the sample edges closest to one another were the areas where the test was carried out. The top samples, which did not undergo any plasma pretreatment, showed a weak adhesion of the deposited films while the pretreated samples (bottom) demonstrated no peeling or separation from the substrate where the tape was applied. The wetting tests showed that the water contact angle went from approximately 120° to 85° for the untreated and treated surfaces, respectively. AFM showed that the surface of the untreated sample was relatively flat with featureless islands compared to the plasma-pretreated sample that comprised of intermingled filaments radiating out from the previously existing islands.

3.4. Titanium nitride deposition

Resultant TiN films were ≈150 nm thick and were composed of (002) and (111) TiN crystals (by XRD). The films deposited with the e-beam-generated plasma showed an increase in the relative amount of (002) crystals from 20% to 27% of the total composition. The AFM analysis over various (4 μm^2) regions showed characteristically shorter and broader grains for the magnetron+e-beam plasma grown films as shown in Fig. 5. These AFM results were further analyzed to produce the peak height distributions shown in Fig. 6, which show most probable peak heights of ≈18 and 13 nm with root-mean-square roughnesses of 4.01 and 2.57 nm for the magnetron and magnetron+e-beam plasma grown films, respectively.

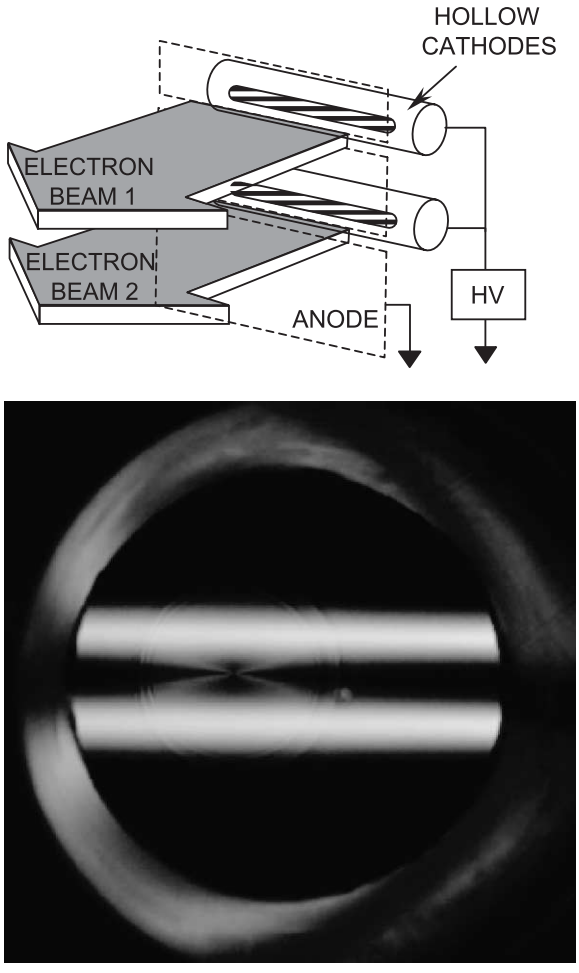

Fig. 7. Schematic (top) and photograph (bottom) of dual e-beam produced plasma system. The center-to-center separation of the e-beams was 5 cm.

3.5. Dual LAPPS system

A plasma source that consists of two e-beams was designed and is presently being tested in our laboratory for double-sided processing applications. These two e-beams are typically operated in parallel from the same power supply with similar currents (≈1 mA/cm^2 cathode operating current), but can be independently addressed as well. A schematic and photograph of the dual e-beam system is shown in Fig. 7. The width (into the page) of each source was 12 cm and the center-to-center separation of the e-beams was 5 cm.

4. Discussion

Plasmas produced by e-beams are quite different than conventional discharges. Their primary advantages for materials applications are (1) low temperature plasma electrons, (2) operational independence from plasma gas composition, and (3) the plasma production efficiency and inherent scalability. All of these advantages have been demonstrated and discussed at length in the literature (see Refs. [1–6]) and will be briefly reiterated here. The resultant low electron temperatures and internal fields are due to the fact that plasma electrons are a by-product of the e-beam ionization process and the plasma sustenance is not driven by the plasma electron distribution. These points are illustrated in Fig. 3, inset, which shows extremely low ion energies at the substrate surface, indicative of low plasma potentials and therefore low electron temperatures. Since ionization is initiated by the electron beam instead of the plasma electrons, plasma production is independent of the gas composition due to the fact that the electron-impact ionization cross sections are basically the same for all gases at kilovolt energies. The ionization by the electron beam also takes only about twice the ionization energy of the target gas molecule [11] (≈30 eV/electron-ion pair), making the ionization process far more efficient compared to conventional discharges that heat the plasma electrons for ionization (hundreds of eV/electron-ion pair [12]). The gas independence and high efficiency of e-beam ionization are fundamental properties of these plasma systems. Together with these attributes and the simplicity of using [high voltage] hollow cathodes for the electron beam production,

increasing the scale of these plasma sources has been predictable and straightforward (see Ref. [6]).

4.1. Stainless steel nitriding

By nitriding the surface of stainless steel at low temperature (≤450 °C), the intrinsic corrosion-resistant properties of the stainless steel are preserved and the surface becomes much harder due to the nitride layer. The nitriding results of these experiments with little optimization are comparable with those in the recent literature [13,14] and considerably faster than standard techniques using rf and dc glow discharges (see Ref. [7] and the references therein). The attractiveness of the e-beam-generated plasma system is further illustrated by the activation energy of 1.4 eV/atom determined for the nitriding process. This activation energy was significantly lower than the value of 1.87 eV/atom for N diffusion in AISI 316 measured by other workers [15], suggesting that e-beam-generated plasmas are rich in active nitriding species such as atomic nitrogen (N). Furthermore, the effective diffusion coefficient [16] (D_0) is 5.7 cm^2/s, similar to previous stainless steel results [17] at higher temperatures. Instead of increased temperatures, which can result in unwanted islands of chrome nitride (CrN), the N diffusivity can be increased by the high flux of nitrogen atoms produced by the e-beam generated plasma. A portion of the high N flux will rapidly occupy the surface chromium atoms and allow the remainder of the nitrogen flux to diffuse through the alloy as if it were pure γ-Fe. The expanded substrate lattice can in turn further enhance the N diffusivity (see Williamson et al. [18] and references contained therein).

The measurable fundamental differences in the present experiments were the large flux of atomic ions and low electron temperatures, compared to the other systems that were dominated by fluxes of molecular ions and high plasma electron temperatures. In these experiments, the abundance of low temperature plasma electrons could rapidly recombine with the molecular ions and reduce their flux to the substrate. This allowed the flux of the two nitrogen ion species to become comparable, unlike other nitriding systems. The atomic ion was therefore considered critical in the formation of the nitrided layer because (1) the increased energy delivered to the substrate surface and (2) it is atomic nitrogen that adsorbs and diffuses into the bulk to promote the nitride layer growth. The IEDFs in Fig. 3 show that the atomic ions arrive at the surface with the full sheath voltage unlike the molecular ions, which lose a significant portion of their acquired sheath-drop energy to charge exchange collisions [19] within the sheath. At the −350 Vdc bias applied in the nitriding experiments, only the atomic ions are capable of sputtering unwanted oxides that inhibit the nitride layer growth. The fact that e-beam produced plasmas in diatomic gases can supply predominantly atomic [4] ions to the workpiece makes it an attractive system for plasma nitriding of materials.

4.2. Polymer pretreatment

The ‘pretreatment’ of the substrates for increased adhesion properties has been discussed widely in the literature [20,21], for applications such as electromagnetic interference shielding, decorative coatings and diffusion barrier coatings. These tests were conducted to demonstrate the non-destructive nature of the e-beam generated plasma source (due to the low energy ions and electrons) on a more delicate substrate while still producing a viable pretreatment process. The excessive processing times showed no overtly deleterious effects to the surface, and significantly improved the interface between the substrate and the capping metal layer.

Chemically, plasma pretreatments are responsible for creating a broad variety of oxygen-containing groups on the fluorocarbon surface, which are known to increase the adhesion of metals through the large metal-oxide bond strengths. Physically, simple sputtering (i.e. roughening) of the surface results in a dramatic increase in surface area and perhaps more importantly, a varying surface normal that requires additional force to remove the metal film [22]. These physical attributes are generally believed to be the primary mechanism for increasing the adhesion of metals to fluoropolymeric materials. From the AFM measurements and the fact that the adhesion of both the copper and aluminum films were increased, the dominant mechanism for the improved adhesion in these experiments appeared to be the [physical] surface morphology rather than surface chemistry, considering that copper is a relatively inert material compared to aluminum.

The tape tests did provide an upper bound on the adhesion performance; Chen et al. [22] determined the peel strength of materials passing the test to be at least 10 g/mm. (The accepted peel strength for the electronics packaging industry is 40 g/mm.) However, the effect of surface chemistry cannot be quantified with the present experiments. The e-beam generated oxygen plasma transformed Teflon® from a non-wetting material (θ>100°) to a wettable material, even after exposure to atmosphere over several hours. However, the observed change in surface energy may be due to a chemically modified surface or finer changes in surface morphology, which were undetected here. The exact determination of the surface chemistry in these experiments remains an uncertain issue and requires more advanced surface analysis techniques to definitively determine the actual chemical groups at the surfaces.

4.3. Titanium nitride deposition

Assuming that the neutral titanium flux from the magnetron was constant in all depositions, the reactive plasma species (neutral and charged nitrogen) were the variable quantities between the two plasma systems used in the TiN deposition experiments. While the total ion current to the substrate was held constant for both deposition

experiments and the substrate bias was fairly low (50 Vdc), only the composition of the ion flux was significantly changed with the e-beam + magnetron system. As discussed previously, the e-beam generated plasmas provide comparable atomic and molecular ion fluxes to the substrate. Furthermore, the low energy plasma electrons from the e-beam generated plasma are free to recombine with the molecular ions generated by the magnetron source to create an additional source of neutral nitrogen atoms. Although the experimental observations are limited, they agree with surface kinetic arguments [23,24] which showed that an increase in atomic nitrogen flux should promote the growth of (002) grains over (111) grains during competitive texture evolution. Furthermore, the (002) oriented grains exhibit a faster lateral growth than (111) grains [25] and the preferred growth of (002) oriented crystals is typically accompanied by reduced film porosity. These film morphology characteristics are also illustrated in the AFM results from Figs. 5 and 6. Although there was only a 7% increase in the amount of (002) present in the film grown with the e-beam produced plasma, significantly lower average grain heights (from 18 to 13 nm) and film roughness (from 4.01 to 2.57 nm) were observed. Both of these traits are consistent with an increased number density of shorter, broader islands of the (002) grains, and thus a lower film porosity. Therefore, from the additional N fluxes provided by the e-beam produced plasma system there was a consistent transition from a (111) texture to a (002) texture in the TiN film growth that included a significant reduction in surface roughness and grain height. Since the ion energy (stage bias) and current was held constant in these experiments, the observed effects can be directly correlated to the ion composition to the surface. The specific impact of ion versus neutral atomic N on TiN film growth is an area of current research in our laboratory.

4.4. Dual LAPPS system

While still in the testing phase, the dual e-beam-generated system in Fig. 7 shows a tremendous amount of promise in materials applications. With the collimating magnetic field already in place for the original e-beam, the implementation of the second cathode was straightforward and added little to the power consumption of the overall system.

Present systems for double-sided processing either rely on batch processing that physically turns over the substrate (and subsequently repeats the process) or suspends the substrate off of the processing stage. The side of the suspended substrate away from the plasma source must then rely on the diffusion of the reactive plasma species in the gas phase, which may cause significant discrepancies in process repeatability and uniformity on both surfaces. With identical plasmas on both sides of the substrate operating simultaneously, such issues may be avoidable.

5. Summary and conclusions

Electron-beam-generated plasmas were used in various surface modification applications. These plasma sources demonstrated considerable flexibility for modifying materials alone and when coupled with sputter magnetron sources. When used alone, the absence of high plasma electron temperatures (and therefore large plasma potentials) allows a variety of processing conditions without sacrificing flux of reactive charged or neutral species. This work demonstrated the important attributes of ion energy control and ion flux composition in plasma processing environment.

Competitive stainless steel nitriding rates (up to 20 μm/$h^{1/2}$) were obtained below 462 °C by providing a significantly higher flux of atomic nitrogen ions from the plasma in a pure nitrogen background. These rates were accompanied by a low process activation energy of 1.4 eV/atom at modest ion energies (350 eV). At these processing conditions, the high corrosion resistance of the bulk stainless steel was preserved with an increased final surface hardness of the nitride (15.5 GPa).

The e-beam-generated oxygen plasma treatment improved the adhesion of aluminum and copper films on Teflon® when subjected to a standard tape test, with no noticeable negative effects. Modification of the Teflon® surface morphology was directly observed after treatment and considered the dominant factor in the increased film adhesion, although chemical activation of surface could be suggested by the reduction of the water contact angle after plasma treatment. Additional tests that are more chemically sensitive would be necessary to quantitatively determine the roles of each mechanism in these experiments and to pinpoint the actual metal bonding strength, believed to be >10 g/mm from the present tests.

The incorporation of an e-beam plasma source during reactive sputtering of TiN revealed that film microstructure could be controlled by the ion flux composition, with an increased atomic nitrogen flux corresponding to an increase in (002) orientation for TiN. The preferential growth of the (002) orientation also resulted in broader features, smoother microstructures and thereby lower porosity of the films, as seen and predicted by others. The possible role of the neutral nitrogen atoms produced is currently an area of active research.

The present experiments were detailed proof-of-concept tests for the practicality of applying e-beam-generated plasmas broadly in materials applications. Aspects also being presently explored are the utility of the dual-beam plasma source for double-sided processing and the modulated nature of all of these plasma sources. Damage-free double-sided processing could present tremendous advantages in fragile material processing with half the processing time of current methods whereas modulated plasmas offer advantages in process space [26] not always accessible with continuous plasma sources. However, more comprehensive

designs-of-experiments are necessary to optimize the processes. These advanced approaches offer exciting avenues for the systems discussed here.

Acknowledgements

CM appreciated the support of the American Society of Engineering Education. The authors are grateful to Drs. I.L. Singer, A. Piqué and S. B. Qadri of NRL for access to materials characterization equipment and encouraging conversations. The technical assistance of Anthony Noll (NRL) and Robert Lanham (SFA, Lanham, MD) was also greatly appreciated. The Office of Naval Research supported this work.

References

[1] R.F. Fernsler, W.M. Manheimer, R.A. Meger, J. Mathew, D.P. Murphy, R.E. Pechacek, J.A. Gregor, Phys. Plasmas 5 (1998) 2137.
[2] W.M. Manheimer, R.F. Fernsler, M. Lampe, R.A. Meger, Plasma Sources Sci. Technol. 9 (2000) 370.
[3] D. Leonhardt, S.G. Walton, D.D. Blackwell, W.E. Amatucci, D.P. Murphy, R.F. Fernsler, R.A. Meger, J. Vac. Sci. Technol., A, Vac. Surf. Films 19 (2001) 1367.
[4] S.G. Walton, D. Leonhardt, D.D. Blackwell, D.P. Murphy, R.F. Fernsler, R.A. Meger, J. Vac. Sci. Technol., A, Vac. Surf. Films 19 (2001) 1325.
[5] D. Leonhardt, Vac. Technol. Coat. (2001 November) 24.
[6] D. Leonhardt, C. Muratore, S.G. Walton, D.D. Blackwell, R.F. Fernsler, R.A. Meger, Surf. Coat. Technol. 177–178 (2004) 682.
[7] C. Muratore, D. Leonhardt, S.G. Walton, D.D. Blackwell, R.F. Fernsler, R.A. Meger, Surf. Coat. Technol. 186 (2004) 40.
[8] C. Muratore, S.G. Walton, R.F. Fernsler, D. Leonhardt, D.D. Blackwell, R.A. Meger, J. Vac. Sci. Technol. A 22 (2004) 1530.
[9] AIMCAL procedure for qualitatively determining metal adhesion, TP-104-87, in: Eldridge M. Mount II (Ed.), Association of Industrial Metallizers, Coaters and Laminators (AIMCAL) Metallizing Technical Reference, 3rd ed., 2001 (August).
[10] D. Leonhardt, et al., Plasma Sources Technol., (submitted for publication).
[11] L. Christophorou, Atomic and Molecular Radiation Physics, Wiley Interscience, New York, 1971.
[12] M.A. Lieberman, A.J. Lichtenberg, Principles of Plasma Discharges and Materials Processing, Wiley Interscience, New York, 1994, p. 81.
[13] J.M. Priest, M.J. Baldwin, M.P. Fewell, S.C. Haydon, G.A. Collins, K.T. Short, J. Tendys, Thin Solid Films 354 (1999) 113.
[14] E.I. Meletis, Surf. Coat. Technol. 149 (2002) 95.
[15] J. Hirovonen, A. Anttila, Appl. Phys. Lett. 46 (1985) 835.
[16] The diffusion constant is simply estimated from $D_0=d^2\exp[E_a/kT]/t$ where d is the thickness of the layer, t is the exposure time and E_a is the experimentally determined activation energy.
[17] A. Kuhl, D. Bergner, H.-J. Ullrich, M. Schlaubitz, P. Karduck, Mikrochim. Acta 107 (1992) 295.
[18] D.L. Williamson, O. Ozturk, R. Wei, P.J. Wilbur, Surf. Coat. Technol. 65 (1994) 15.
[19] A.V. Phelps, The resonant charge exchange cross section of 3.1×10^{-15} cm^{-2}, J. Phys. Chem. Ref. Data 20 (1991) 557.
[20] K. De Bruyn, M. Van Stappen, H. De Deurwaerder, L. Rouxhet, J.P. Celis, Surf. Coat. Technol. 163–164 (2003) 710.
[21] J.M. Grace, L.J. Gerenser, J. Dispers. Sci. Technol. 24 (2003) 305–341.
[22] C.-A. Chang, Appl. Phys. Lett. 51 (1987) 1236;
C.-A. Chang, Y.-K. Kim, S.S. Lee, in: K.L. Mittal (Ed.), Metallized Plastics, Marcel Dekker, New York, 1998.
[23] D. Gall, S. Kodambaka, M.A. Wall, I. Petrov, J.E. Greene, J. Appl. Phys. 93 (2003) 9086.
[24] C.-S. Shin, S. Rudenja, D. Gall, N. Hellgren, T.-Y. Lee, I. Petrov, J.E. Greene, J. Appl. Phys. 95 (2004) 356.
[25] J.-S. Chun, I. Petrov, J.E. Greene, J. Appl. Phys. 86 (1999) 3633.
[26] L. Bárdoš, H. Baránková, Vac. Technol. Coat. (2001 September) 47.